Rod-like fluorescent halloysite nanotubes-silica composites: a novel colloidal system

R. Sánchez[a], B.M. Marín-Santibáñez[b], J. Pérez-González[c], F. Rodríguez-González[d], and H.J. Dorantes-Rosales[e]

[a]*Facultad de Física, Universidad Veracruzana, Circuito Gonzalo Aguirre Beltrán s/n, Zona Universitaria, Xalapa 91000, Veracruz, Mexico.*

[b]*Sección de Estudios de Posgrado e Investigación, Escuela Superior de Ingeniería Química e Industrias Extractivas, Instituto Politécnico Nacional, U.P.A.L.M. C.P. 07738, Col. S. P. Zacatenco, Del. Gustavo A. Madero, México D.F., México.*

[c]*Laboratorio de Reología y Física de la Materia Blanda, Escuela Superior de Física y Matemáticas, Instituto Politécnico Nacional, U.P.A.L.M. C.P. 07730, Col. S. P. Zacatenco, Del. Gustavo A. Madero, México D.F., México.*

[d]*Departamento de Biotecnología, Centro de Desarrollo de Productos Bióticos, Instituto Politécnico Nacional, C.P. 62731, Col. San Isidro, Yautepec, Morelos, México.*

[e]*Departamento de Metalurgia y Materiales, Escuela Superior de Ingeniería Química e Industrias Extractivas, Instituto Politécnico Nacional, U.P.A.L.M. C.P. 07738, Col. S.P. Zacatenco, Del. Gustavo A. Madero, México D.F., México.*

Received 17 October 2014; accepted 21 January 2015

An inexpensive novel method to produce a rod-like fluorescent colloidal system is presented in this work. The system consists of core-shell particles synthesized by using halloysite nanotubes as cores, and silica layers as shells on their surfaces. Unlike traditional protocols for producing silica core-shell particles, the method used in this work does not require a coupling agent. In addition, a fluorescent dye was incorporated to produce fluorescent composites. Due to their resulting morphology and the possibility of incorporating a fluorescent dye, they constitute a promising new colloidal model system for studying the physics of anisotropic colloidal suspensions experimentally, as well as a potential source of new materials.

Keywords: Nanoclay composites; core-shell particles; halloysite nanotubes; colloidal rods.

PACS: 81.07.De; 81.05.Pj; 83.80.Hj

1. Introduction

Colloidal composites such as core-shell nanoparticles have been widely studied in recent years, since they are of great relevance for applications as well as of fundamental scientific interest, including for the development of new experimental model systems. However, with some exceptions [1-3], there is a relative dearth of elongated colloidal model systems and many of the synthesis methods in the literature rely on comparatively cumbersome processes based on colloidal aggregation [4-5]. Furthermore, published methods for the production of rod-like elongated particles typically result in modest aspect ratios. Nevertheless, rod-like colloids with high aspect ratios are of considerable interest as constituents of anisotropic materials and suspensions, as analogues of molecular systems like liquid crystals and of some biological systems, and in their own right, due to the phase behavior of systems such as sterically stabilized sepiolite clay particles [6].

Halloysite nanotubes (HNTs) are naturally-occurring aluminosilicates [7,8] chemically similar to kaolin [7,9-13], and are mined from deposits in China, the United States and Brazil, among others [10]. They are inexpensive compared to carbon nanotubes [10,12,14] - an important practical consideration if a tubular or rod-like morphology is required and the specific chemistry is of secondary importance, for instance in model systems for colloid physics studies. In addition, they are non-toxic, biocompatible [15,16] and readily processed by conventional means without requiring exfoliation [17]. HNTs typically have a length of 1-15 μm, an inner diameter (lumen) of 10-30 nm and an outer diameter of 50-70 nm [11]. In recent years this nanoclay has attracted considerable interest for the production of a variety of composites [8]. Research has mostly focused either on encapsulation within the lumen [18-20], or on composites, mainly with polymers [21].

A halloysite nanotube's outermost layer consists of silica and the innermost one consists of alumina [21], which suggests that core-shell syntheses appropriate for pure silica cores are likely suitable for HNT substrates. Silica has various useful features such as high resistance to corrosion and non-toxicity, and produces surfaces than can be easily modified chemically.

In this work, we present a simple novel method for preparing rod-like fluorescent and non-fluorescent colloidal systems using HNTs, as well as their microscopic characterization.

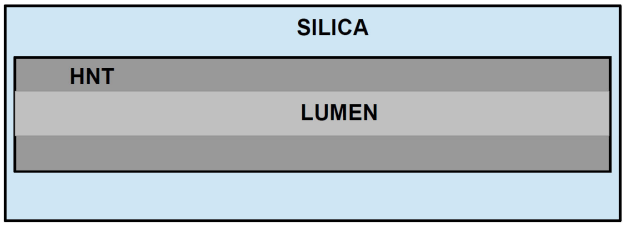

FIGURE 1. The desired composite is shown schematically. It consists of a halloysite core and non-fluorescent outer silica shells.

2. Materials and Methods

2.1. Overview

The single-pot procedure used in the present work is based on the well-known Stöber method [22,23], a reaction between tetraethyl orthosilicate (TEOS) and water consisting of hydrolysis followed by condensation, which produces silica and ethanol ($Si(OC_2H_5)_4 + 2H_2O \rightarrow SiO_2 + 4C_2H_5OH$). Instead of synthesizing silica shells on spherical silica cores, in the present work two-component and three-component rod-like core-shell systems were prepared. They consist of HNT cores with silica shells for the two-component system, and HNT cores with silica shells and a fluorescent layer for the three-component one (see Fig. 1). Unlike traditional Stöber-based protocols for producing fluorescent particles, our method does not require a coupling agent. Note that the halloysite itself does not react, but instead provides a substrate for the synthesized silica, just as in typical core-shell silica syntheses a silica core provides a substrate for subsequent silica layers.

2.2. Sample preparation

Halloysite from Sigma-Aldrich (purity in the 90-100 % range according to the supplier) was dispersed in an aqueous sodium hexametaphosphate (0.05 wt %) solution at 10 wt % under sonication. Large particles were separated by sedimentation achieved by centrifugation for 2.5 min at 2400 rpm, and subsequent decantation. The nanoclay was then dried, repeatedly ground with pestle and mortar, and sifted using a 37 μm sieve prior to use. All other materials were used as received. Unless specified otherwise in Table I, materials were of reagent grade, 98 %. Typical amounts used for the initial reaction, carried out at room temperature with stirring for a minimum of 4 hours, are shown in Table I.

Further layers of silica were synthesized by additions of TEOS and water, typically $\sim$ 0.15 g and $\sim$ 0.03 g respectively, and the reaction was allowed to proceed for a minimum of two hours, forming the outer silica layer shown schematically in Fig. 1. Water was added last in all procedures; water adsorbed onto the HNTs (we estimate an upper bound of approximately 5 % water content in the halloysite used) is not included in Table I. Six shells were synthesized for the results presented. Once the desired number of shells had been synthesized, the product was decanted, dispersed by 5 minutes of sonication and diluted in ethanol. The particles were allowed to sediment and the supernatant was replaced with clean ethanol. The particles were then re-dispersed manually and washed with clean ethanol, a procedure that was repeated three times.

TABLE I. Ingredients for initial step of synthesis.

Substance	Amount (g)	Supplier & notes
HNTs	0.4983	Aldrich 685445
Fluorescein	0.0016	Aldrich F2456
Ethanol	1.9124	Reasol, anhydrous
TEOS	0.1431	Aldrich 86578
H_2O	1.0204	Tridistilled
NH_4OH(aq)	0.4935	J. T. Baker 9721

2.3. Characterization

Once washed and dispersed in clean ethanol, a sample of the fluorescent composites was allowed to evaporate on a microscope slide and was examined using dark field optical microscopy with white light and fluorescence microscopy with blue light excitation using a Nikon LV100D microscope.

Fluorescent composites were also characterized by scanning electron microscopy (SEM) using a FEI Sirion machine. The composites were also dispersed in methanol by 15 minutes of sonication before being placed on a graphite grid and examined by electron transmission microscopy (TEM) using a JEOL J2000FX machine.

UV-vis spectroscopy of the composites was carried out using dilute suspensions in ethanol and a Lambda 25 Perkin Elmer spectrometer, using ethanol for the blank.

Colloidal stability of the composites in ethanol was assessed in terms of their sedimentation time, which was indirectly obtained from transmitted light measurements in silica-free HNTs and in non-fluorescent composite suspensions, respectively. The particles were dispersed in ethanol at a fixed concentration of 0.2 mg/ml, and were then analyzed using a visible light spectrometer (Spectronic 20, Bausch & Lomb) at a wavelength of 530 nm. Prior to testing, the original composite suspension was re-dispersed manually in ethanol and the supernatant was removed to reduce the presence of silica spheres, a procedure that was also repeated three times.

3. Results and Discussion

Figure 2 shows that the synthesis results in both rods (of length and aspect ratio consistent with composites with HNT cores and silica outer shells) and silica spheres. Fluorescein was successfully caged when the first silica layer was synthesized, as follows from the fact that the composites are fluorescent, as can be seen in Fig. 3, which shows the washed composite displaying the characteristic green color of fluorescein when illuminated with blue light. The presence of

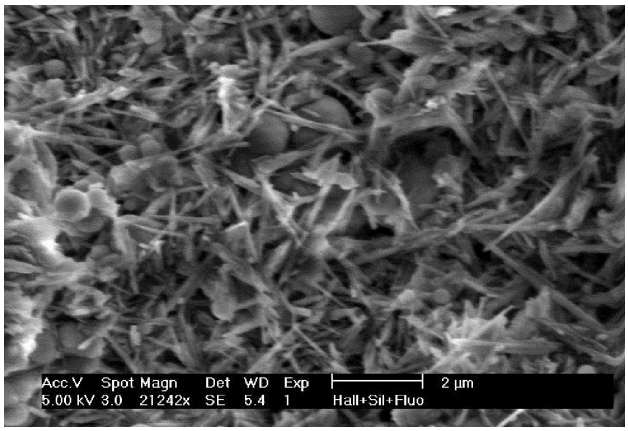

FIGURE 2. SEM image of fluorescent halloysite-silica composites. Both core-shell structures (appearing as rods) and silica spheres arising from secondary nucleation in the bulk solvent are formed.

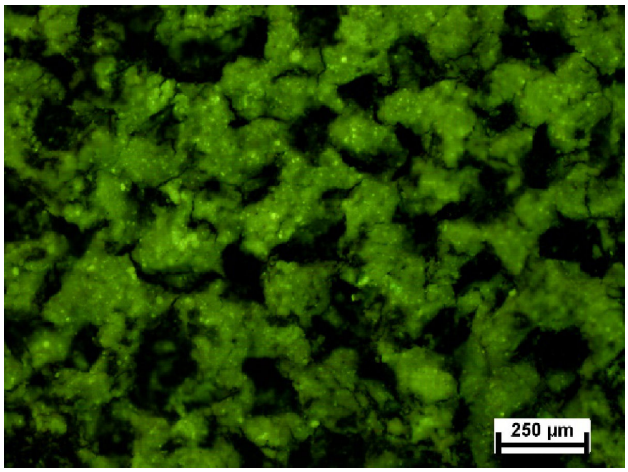

FIGURE 3. Fluorescence microscopy image of fluorescent halloysite-silica composites. The fluorescent regions consists mainly of composites, and the bright spots are thought to be silica spheres. The presence of dark regions suggests that little or no fluorescein was present in the bulk ethanol.

dark regions without fluorescein residues from solvent evaporation on the microscope slide suggests that the protocol is highly efficient in terms of incorporating fluorescein. Moreover, UV-vis spectra of the composites, shown in Fig. 4, confirm the presence of silica (large absorbances at low wavelengths), HNTs (peaks at ~ 380 nm and at ~ 425 nm) and, for fluorescent composites, of fluorescein (see insets). The precise amount of fluorescein incorporated in a particular sample may be determined by using techniques such as Surface-Enhanced Raman Spectroscopy (SERS) [24,25]. Such a determination, however, is beyond the scope of this work.

Due to the water naturally found on the HNTs, the environment immediately adjacent to their surfaces is at least partly aqueous. In pH 7 water, according to the respective adsorption isotherms, the amount of fluorescein adsorbed on alumina surfaces is of the order of 14 times that adsorbed on silica at similar concentrations [26]. Therefore, it is likely that fluorescein adsorbs mostly onto the alumina surface

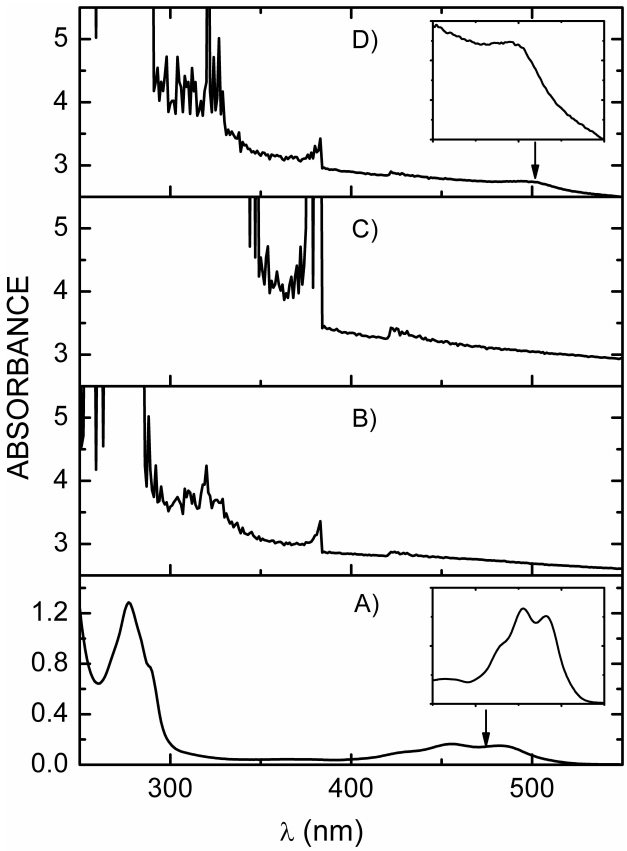

FIGURE 4. UV-vis spectra for fluorescein (A), HNTs (B), non-fluorescent composites (C) and fluorescent composites (D). The insets show peaks due to fluorescein excitation. Saturated data points are not shown.

within the lumen (*i.e.* onto the HNTs' inner surfaces), and thus needs no coupling agent, and is confined as the silica layers form. In order to shed light on the plausibility of this mechanism, a Stöber synthesis was carried out with a similar protocol, but in the absence of halloysite. It did not result in incorporation of fluorescein within the synthesized silica, showing that the silica surface does not incorporate fluorescein without a coupling agent.

Figures 5 and 6 exhibit TEM images of fluorescent core-shell particles. Figure 5 displays an HNT core surrounded by a thin, probably water-rich, layer, and finally a thick outer shell consisting of multiple silica layers. The image in Fig. 6, depicting a composite particle with partially-formed silica shells, shows that silica layers of comparable thickness are indeed formed for each addition of TEOS and water.

As boundaries between individual silica layers in this outer shell cannot be distinguished, the average thickness of individual silica layers was estimated from Fig. 5 assuming that all layer have similar thickness, yielding a value of approximately 5 nm. This value is well below the corresponding calculation obtained by assuming perfectly efficient conversion from TEOS to silica layers on the composites, which, neglecting end effects and polydispersity, would be

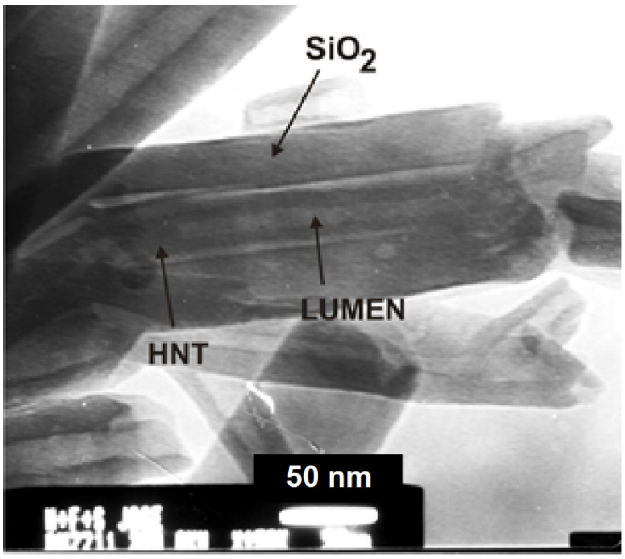

FIGURE 5. TEM image of fluorescent halloysite-silica composites. The various constituents of this core-shell system are clearly visible, even the aqueous layer. The lack of a visible layer between the HNT proper and its lumen suggests the amount of water on the HNT's inner surface is much smaller than that on its outside surface. For this particular composite, the silica layer has an average thickness of 30.84 $\pm$ 1.71 nm, and the HNT has an outer diameter of 31.98 $\pm$ 0.89 nm and a lumen of $\sim$ 8.4 nm. The scale bar measures 50 nm.

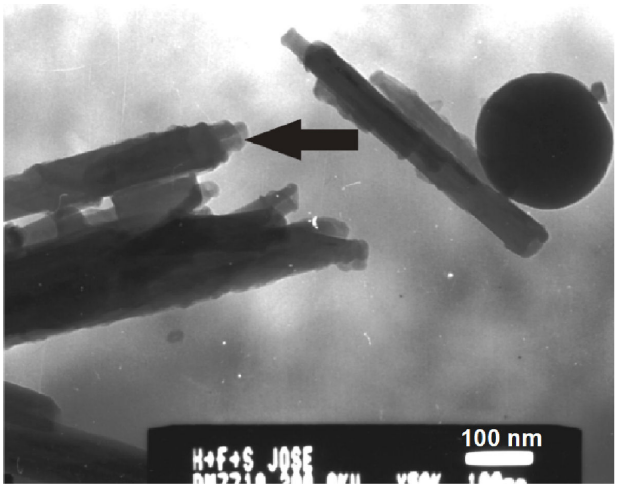

FIGURE 6. TEM image of fluorescent halloysite-silica composites. For the composite particle indicated by the arrow, the partially-formed multiple silica layers can be readily distinguished. The sphere near the right hand corner is a silica sphere resulting from secondary nucleation in the bulk. The scale bar measures 100 nm.

$\sim$ 40 nm in thickness. The "missing" silica is likely found in the spheres visible in Fig. 3. If required, it may be possible to prevent the formation of these spheres by using a much slower experimental protocol to prevent secondary nucleation in the bulk solvent, although yields may be much smaller for convenient reaction times. The TEM image in Fig. 6, depicting a composite particle with partially-formed silica shells, shows that silica layers of comparable thickness are indeed formed for each addition of TEOS and water.

Figures 5 and 6 show that composite length is governed entirely by HNT length and thus the length distribution is essentially that of the HNT cores (see Introduction), whereas outer diameter polydispersity is $\sim$ 41 %.

The experimental colloidal phase behavior of composites synthesized using our protocol, with suitable modifications, may be used to compare with simulational work on rigid spherocylinders with different aspect ratios [27-31]. Our particles have the advantage that the cores would appear as bright rods in fluorescent imaging, simplifying the characterization of their positions and orientations, and thus of phase transitions such as isotropic-nematic, and of their rotational dynamics. In this context, producing fluorescent colloidal rods is advantageous for their study using techniques such as confocal microscopy [32]. The fact that the outer silica shell does not fluoresce should reduce optical aberrations that, even if modest, can distort the apparent physics of a system [33], thus enhancing the accuracy of tracked positions and orientations.

The polydispersity of these naturally occurring HNTs may be reduced by fractionation if a lower polydispersity is desired for the final product, though polydispersity does not hinder the synthesis. Reducing polydispersity as well as secondary nucleation of silica spheres are the subjects of ongoing work.

In terms of aggregation, colloidal silica is stable in common solvents such as water and ethanol. Our composites conform to such behavior as shown by the light transmittance measurements plotted in Fig. 7. This indicates that the silica-free HNTs have consistently higher transmittances and thus

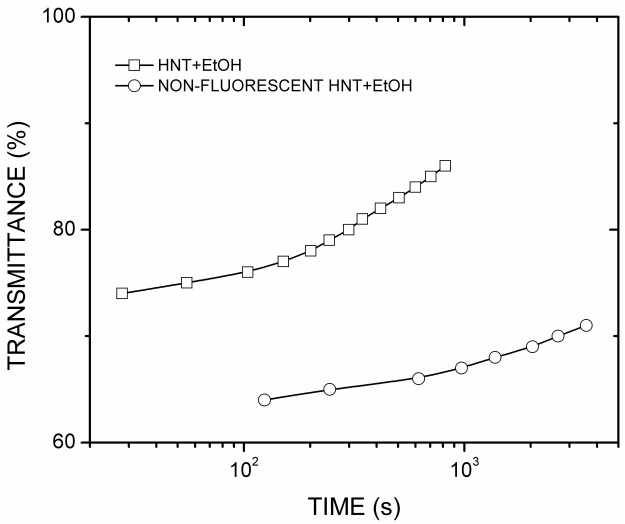

FIGURE 7. Light transmittances, as a function of time, of non-fluorescent core-shell composites (circles) and of HNTs without silica (squares). The silica-free HNTs have consistently higher transmittances, showing that the composite particle suspensions are reasonably stable; long sedimentation times are advantageous for rheological studies.

must be sedimenting more rapidly than the silica-covered HNTs. Longer sedimentation times are advantageous, for example, for rheological studies, which are an intended future application of this system.

Apart from the suggested use as model colloids, the particles produced in this work could be used, for example, to manufacture novel ceramics for applications such as filtering, for which the pore size would be determined by the number and thickness of the silica layers. Furthermore, functionalized silica nanoparticles are of biomedical and biological interest [34,35], and our composites may be useful specifically as fluorescent nanoprobes [36], for example for studying the uptake of highly elongated nanoparticles. Separately, silica's chemical stability could be very useful for certain applications if undesirable substances are encapsulated within the HNTs, as the outside silica layers would safely confine them by sealing the HNTs.

4. Conclusions

Rod-like core-shell halloysite-silica composites, whose morphology is governed by the halloysite cores, have been successfully produced and characterized on a microscopic scale. These particles constitute a promising model system for fields such as colloidal physics due to the possibility of incorporating a fluorescent dye and due to their rod-like morphology and high aspect ratio. Furthermore, due to the properties of their outer surfaces, they are also a promising component of novel materials. The results obtained strongly suggest that core-shell synthesis techniques applicable to silica cores in ethanol can be carried out with halloysite cores, and may not always require the use of coupling agents due to the possibility of encapsulation. This potentially means that such methodologies can be applied to the production of novel colloidal suspensions and ceramics based on halloysite.

Acknowledgments

RS acknowledges Consejo Nacional de Ciencia y Tecnología support (Retención 174462) while carrying out part of the present work, and acknowledges use of SARA-UV facilities at Xico, Veracruz. BMMS, JPG, FRG and HJDR are COFAA-EDI fellows. The authors also acknowledge technical assistance from K. García-Morales.

1. S. Sacanna, L. Rossi, B.W.M. Kuipers, and A.P. Philipse, *Langmuir* **22** (2006) 1822-1827.
2. Q. Dong *et al*., *J. Ceram. Soc. Jpn.* **117** (2009) 245-248.
3. A. Kuijk, A. van Blaaderen, and A. Imhof, *J. Am. Chem. Soc.* **133** (2011) 2346-2349.
4. H.K. Choi, S.H. Im, and O.O. Park, *Langmuir* **26** (2010) 12500-12504.
5. Q. Zhang, S. Zeng, B. Lin, and J. Qin, *J. Mater. Chem.* **21** (2011) 2466-2469.
6. Z.X. Zhang and J.S. van Duijneveldt, *J. Chem. Phys.* **124** (2006) 154910.
7. D.C.O. Marney *et al*., *Polym. Degrad. Stab.* **93** (2008) 1971-1978.
8. M. Du, B. Guo, J. Wan, Q. Zou, and D. Jia, *J. Polym. Res*. **17** (2010) 109-118.
9. G. Tari, I. Bobos, C.S.F. Gomes, and J.M.F. Ferreira, *J. Colloid Interface Sci.* **210** (1999) 360-366.
10. M. Du, B. Guo, and D. Jia, *Eur. Polym. J.* **42** (2006) 1362-1369.
11. M. Liu, B. Guo, M. Du, X. Cai, and D. Jia, *Nanotechnology* **18** (2007) 455703.
12. N. Ning, Q. Yin, F. Luo, Q. Zhang, R. Du, and Q. Fu, *Polymer* **48** (2007) 7374-7384.
13. S. Rooj, A. Das, V. Thakur, R.N. Mahaling, A. K. Bhowmick, and G. Heinrich, *Mater. Des.* **31** (2010) 2151-2156.
14. Y. Ye, H. Chen, J. Wu, and L. Ye, *Polymer* **48** (2007) 6426-6433.
15. V. Vergaro *et al*., *Biomacromolecules* **11** (2010) 820-826.
16. R. Qi, X. Cao, M. Shen, R. Guo, J. Yu, and X. Shi, *J. Biomater. Sci. Polym. Ed.* **23** (2012) 299-313.
17. H. Ismail, P. Pasbakhsh, M.N.A. Fauzi, and A.A. Bakar, *Polym. Test.* **27** (2008) 841-850.
18. D.G. Shchukin, and H. Mhwald, *Adv. Funct. Mater.* **17** (2007) 1451-1458.
19. M.T. Viseras, C. Aguzzi, P. Cerezo, and C. Viseras, *Microporous Mesoporous Mater.* **108** (2008) 112-116.
20.] E. Abdullayev, R. Price, D. Shchukin, and Y. Lvov, *ACS Appl. Mater. Interfaces* **1** (2009) 1437-1443.
21. Y. Lvov and E. Abdullayev, *Prog. Polym. Sci.* **38** (2013) 1690-1719.
22. W. Stöber and A. Fink, *J. Colloid Interface Sci.* **26** (1968) 62-69.
23. X.D. Wang *et al*., *J. Coll. Interf. Sci.* **341** (2010) 23-29.
24. G. Gouadec, and P. Colomban, *Progr. Crystal Growth Charact. Mater.* **5** (2007) 1-56.
25. L.K. Shrestha, J.S. Wi, J. Williams, M. Akada, and K. Ariga, *J. Nanosci. Nanotechnol.* **14** (2014) 2245-2251.
26. T. Kasnavia, D. Vu, and D.A. Sabatini, *GroundWater* **37** (1999) 376-381.
27. S.C. McGrother, D.C. Williamson, and G. Jackson, *J. Chem. Phys.* **104** (1996) 6755-6771.
28. S.C. McGrother, A. Gil-Villegas, and G. Jackson, *Mol. Phys.* **95** (1998) 657.
29. C. Avendaño, A. Gil-Villegas, and E. González- Tovar, *J. Chem. Phys*. **128** (2008) 044506.
30. S.V. Savenko and M. Dijkstra, *Phys. Rev. E* **70** (2004) 051401.

31. R. Ni, S. Belli, R. van Roij, and M. Dijkstra, *Phys. Rev. Lett.* **105** (2010) 088302.
32. M.C. Jenkins and S.U. Egelhaaf, *Adv. Colloid Interface Sci.* **136** (2008) 65-92.
33. J. Baumgartl, J.L. Arauz-Lara, and C. Bechinger, *Soft Matter* **2** (2006) 631-635.
34. L. Wang, W. Zhao, and W. Tan, *Nano. Res.* **1** (2008) 99-115.
35. A. Bitar, N.M. Ahmad, H. Fessi, and A. Elaissari, *Drug Discov. Today* **17** (2012) 1147-1154.
36. J. Mérian, J. Gravier, F. Navarro, and I. Texier, *Molecules* **17** (2012) 5564-5591.